

The Status of Inelastic Dark Matter

David Tucker-Smith*

*Department of Physics, Williams College,
Williamstown, MA 01267, USA*

Neal Weiner†

*Center for Cosmology and Particle Physics,
Dept. of Physics, New York University,
New York, NY 10003, USA*

and

*Department of Physics, Box 1560,
University of Washington,
Seattle, WA 98195-1560, USA*

(Dated: October 25, 2018)

In light of recent positive results from the DAMA experiment, as well as new null results from CDMS Soudan, Edelweiss, ZEPLIN-I and CRESST, we reexamine the framework of inelastic dark matter with a standard halo. In this framework, which was originally introduced to reconcile tensions between CDMS and DAMA, dark matter particles can scatter off of nuclei only by making a transition to a nearly degenerate state that is roughly 100 keV heavier. We find that recent data significantly constrains the parameter space of the framework, but that there are still regions consistent with all experimental results. Due to the enhanced annual modulation and dramatically different energy dependence in this scenario, we emphasize the need for greater information on the dates of data taking, and on the energy distribution of signal and background. We also study the specific case of “mixed sneutrino” dark matter, and isolate regions of parameter space which are cosmologically interesting for that particular model. A significant improvement in limits by heavy target experiments such as ZEPLIN or CRESST should be able to confirm or exclude the inelastic dark matter scenario in the near future. Within the mixed sneutrino model, an elastic scattering signature should be seen at upcoming germanium experiments, including future results from CDMS Soudan.

In light of the WMAP results [1], our understanding of what we do not know has been placed on very strong footing. The overwhelming majority of the energy density of the universe is of unknown origin, with 23% an unknown dark matter, and 73% a mysterious dark energy. A determination of the nature of these components would represent a remarkable advance in our understanding of the universe. This fact makes the recent DAMA results [2], which use seven years of data to establish a 6.3σ signal consistent with WIMP-nuclei scattering, worthy of particular attention.

One troubling aspect of the DAMA signal has been its apparent disagreement with other experiments, notably CDMS [3], Edelweiss [4], ZEPLIN-I [5, 6], and CRESST [7], when interpreted as evidence of an ordinary WIMP. Efforts to reconcile WIMP search results by modifying the halo profile have met with limited success [8], and possibilities such as spin-dependent interactions seem quite constrained from other sources [9]. Indeed, even the generalized analysis of [10] concludes that it is difficult to reconcile the experiments. However, the class of models considered there does not include the scenario

studied here, in which WIMP scattering off of nuclei is dominantly inelastic.

Inelastic dark matter (iDM) [11] was introduced to explain the tension between the DAMA four year data [12] and CDMS. One reason DAMA and CDMS are consistent in this framework is that iDM favors heavier target nuclei, such as iodine, over germanium. An essential ingredient in testing this framework [11, 13], is therefore the study of additional heavy target experiments. Now that we have additional data from heavy target nuclei, at ZEPLIN-I (Xe), and at CRESST (W), as well as new, stringent limits from CDMS Soudan, it is worth reexamining this scenario to see what parameter space is still allowed.

In the following section, we review the basic features of iDM, what its effects can be on experiments, and possible origins for iDM, namely a heavy Dirac neutrino and a “mixed” sneutrino. In section II, we obtain regions of parameter space presently consistent with existing experiments. In section III, we investigate whether there are allowed regions consistent with mixed-sneutrino dark matter, based on relic abundance calculations.

I. INELASTIC DARK MATTER

The iDM scenario features:

*Electronic address: dtuckers@williams.edu

†Electronic address: neal.weiner@nyu.edu

- A dark matter particle, χ_1 , with zero or highly suppressed elastic scattering cross sections off of nuclei.
- A second state, χ_2 , heavier than χ_1 by an amount $\delta = m_2 - m_1$, which is of the order of a typical halo WIMP kinetic energy. Generally, we need $\delta \sim 100$ keV for weak-scale values of the χ_1 and χ_2 masses.
- An allowed scattering off of nuclei with an inelastic transition of the dark matter particle, i.e., $\chi_1 + n \rightarrow \chi_2 + n$.

Later, we will see that such a peculiar setup can arise naturally, if degenerate states, with elastic scatterings between them, are split by symmetry breaking parameters [14].

The scale of the splitting is an essential feature, because only with $\delta \sim 100$ keV can we have interesting effects in terrestrial experiments. For instance, a Bino, with negligible elastic scattering, could in principle scatter into a Higgsino via Higgs exchange, but in this case the splitting is typically far too large (several GeV) for inelastic scattering to be kinematically allowed. At the other extreme, a particle with negligible splitting compared to typical kinetic energies would essentially scatter as an ordinary WIMP. In the DAMA analysis of this scenario [15], this has been referred to, appropriately and descriptively, as “preferred inelastic scattering.”

A. Consequences of iDM

Broadly speaking, the iDM scenario can have three effects on dark matter experiments:

- An overall suppression of signal, favoring heavier targets over lighter ones.
- An energy-dependent suppression of signal, suppressing rates of low energy events more than those of high energy events.
- An enhancement of the modulated signal relative to the unmodulated signal.

We will see that these features allow the results of DAMA to be reconciled with the results of other WIMP searches.

The central kinematical change is that only those dark matter particles with sufficient incident energy can scatter. This minimum velocity to scatter with a deposited energy E_R is

$$\beta_{min} = \sqrt{\frac{1}{2m_N E_R}} \left(\frac{m_N E_R}{\mu} + \delta \right), \quad (1)$$

where μ is the reduced mass of the iWIMP/target system. In general, there is a broad distribution of velocities in the halo, most commonly considered to be a modified Maxwell-Boltzmann distribution. Therefore, the principle effect at a given experiment is to limit the sensitivity only to a part of the phase space of the halo.

The first simple observation one can make is that the minimum velocity in eq. (1) decreases as one moves to heavier target nuclei. This simple fact alone can reconcile DAMA with light-target experiments, but a full analysis requires us to calculate carefully the event rates at all experiments.

To do this, we follow [11]. The differential rate per unit detector mass is given by

$$\frac{dR}{dE_R} = N_T \frac{\rho_\chi}{m_\chi} \int_{v_{min}} dv v f(v) \frac{d\sigma}{dE_R}. \quad (2)$$

Here N_T is the number of target nuclei per unit mass, ρ_χ is the local density of dark matter particles of mass m_χ , $\frac{d\sigma}{dE_R}$ is the differential cross section for relic-nucleus scattering, and v and $f(v)$ are the relic speed and speed distribution function in the detector rest frame. We take $\rho_\chi = .3$ GeV/cm³.

For spin independent interactions, we can write the differential cross section as

$$\frac{d\sigma}{dE_R} = \frac{m_N \sigma_n (f_p Z + f_n (A - Z))^2}{2v^2 \mu_n^2 f_n^2} F^2(E_R), \quad (3)$$

μ_n is the reduced mass of the nucleon/WIMP system (not *nucleus*/WIMP system), f_n and f_p are the relative coupling strengths to neutrons and protons, and σ_n is the WIMP-neutron cross section at zero momentum transfer, in the elastic ($\delta = 0$) limit. For consistency, we use the Helm form factor [16]

$$F^2(E_r) = \left(\frac{3j_1(qr_0)}{qr_0} \right)^2 e^{-s^2 q^2}, \quad (4)$$

with $q = \sqrt{2m_N E_R}$, $s = 1$ fm, $r_0 = \sqrt{r^2 - 5s^2}$, and $r = 1.2 A^{1/3}$ fm.

In the galactic rest frame, we will use the standard Maxwell-Boltzmann distribution of velocities with $v_{rms} = \sqrt{\frac{3}{2}} v_0$, where we take $v_0 = 200$ km/s for the rotational speed of the local standard of rest. With the recent CDMS Ge result, it is important to be aware of the effect of the finite escape velocity. Details of this cutoff, including its size and the distribution of velocities near it, are very model dependent. As a simple approximation, we will set the differential cross section, as a function of energy, to zero if the minimum velocity exceeds the galactic escape velocity, $\beta_{min}(E_R) > \beta_{esc}$. That is,

$$\frac{d\sigma}{dE_R} \rightarrow \frac{d\sigma}{dE_R} \Theta(\beta_{esc} - \beta_{min}(E_R)). \quad (5)$$

Although this cutoff tends to overestimate the signal when $\beta_{min} \sim \beta_{esc}$, we will not concern ourselves with this here as the details of the galactic cutoff are uncertain. As we will see, the abrupt cutoff produces certain artifacts in the predicted energy spectra, which should be interpreted as signals of cosmological uncertainty. We choose a relatively high value for the escape velocity, $v_{esc} = 730$ km/s

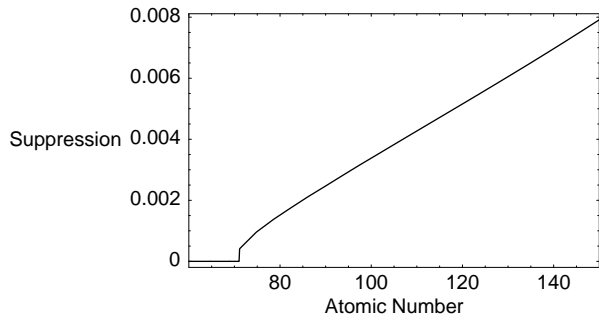


FIG. 1: The suppression of signal in the energy range $10\text{keV} < E_R < 150\text{keV}$ for $m_\chi = 70\text{GeV}$ and $\delta = 100\text{keV}$ as a function of the atomic number of the target.

[17], to obtain the broadest possible region of allowed parameter space.

The Earth moves relative to the galactic rest frame

$$v_e = v_\odot + v_{orb} \cos \gamma \cos(\omega(t - t_0)). \quad (6)$$

In this expression $v_{orb} = 30\text{ km/s}$, $\omega = 2\pi/\text{year}$, $v_\odot = v_0 + 12\text{ km/s}$, $t_0 \simeq \text{June 2nd}$, and $\cos \gamma = .51$. Taking dimensionless variables $\eta = v_e/v_0$ and $x_{min} = v_{min}/v_0$, performing the velocity integration in eq. 2, and applying the cross section formula in eq. 3, one obtains

$$\begin{aligned} \frac{dR}{dE_R} = & \frac{N_T m_N \rho_\chi}{4v_0 m_\chi} F^2(E_R) \frac{\sigma_n}{\mu_n^2} \frac{(f_p Z + f_n(A - Z))^2}{f_n^2} \\ & \times \left(\frac{\text{erf}(x_{min} + \eta) - \text{erf}(x_{min} - \eta)}{\eta} \right) \Theta(\beta_{esc} - \beta_{min}(E_R)). \end{aligned} \quad (7)$$

Notice that the modulation and dependence on δ are entirely encoded in the second line.

At this point we have obtained all of the results needed to illustrate the three basic effects that the inelasticity can have at dark matter experiments.

The simplest of these is the effect on the total rate. Because only a fraction of the velocity space is accessible experimentally, the total rate at an experiment is suppressed considerably. In figure 1, we show the dependence of this effect on the atomic number of the target. This illustrates that heavier targets (such as iodine) can have significantly increased signal over the lighter targets (such as germanium).

However, it is also important to note where this suppression is coming from. While, indeed, the entire energy range is suppressed, the low energy events are suppressed significantly more. We illustrate this in figure 2. This effect tends to favor experiments with higher minimum energies, such as Edelweiss (20 keV) and DAMA (2 keV with a quenching of .09, or roughly 22 keV), over experiments with lower thresholds, such as CDMS (10 keV), ZEPLIN-I (2 keV with a quenching of .2, or roughly 10 keV), and CRESST (12 keV).

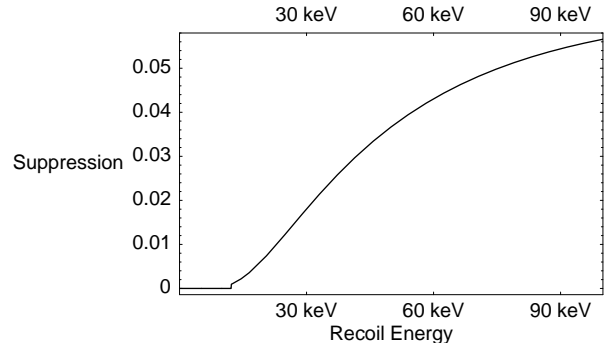


FIG. 2: The suppression of signal as a function of energy at a germanium experiment, with $m_\chi = 120\text{GeV}$ and $\delta = 80\text{keV}$.

The energy dependence of the suppression can produce a substantial spectral distortion of the signal. For instance, while the standard expectation is for the signal to peak at low energies, that need not be the case here, as we show in figures 3a) and b). As stated earlier, the abrupt cutoff in the energy spectrum of the inelastic case is an artifact of the sharp cutoff in the signal for velocities above the escape velocity, and should be properly interpreted as a signal of cosmological uncertainties in the spectrum around the cutoff energy. However, there is less uncertainty in the associated histogram, and the zero signal for sufficiently low energies is a robust result.

Finally, there is the enhancement of the modulation signal compared with the unmodulated component. Usually, it is safe to assume that the modulation will not exceed several percent of the unmodulated signal. However, in the inelastic scenario, we see in figure 4 that the modulated signal can reach nearly 30% of the unmodulated signal, improving the comparison of DAMA's modulation result to the unmodulated null results of the other experiments.

Note that the effects of the inelasticity are independent of whether the interactions are spin-independent or spin-dependent. However, while inelastic spin-dependent interactions are a logical possibility, there is good reason to expect that any spin-dependent contributions that are present will be elastic (for instance, in the axial coupling of a fermion, each Majorana component couples to itself, rather than the two components coupling to each other). For this reason, spin-dependent dark matter probes are not especially sensitive to this scenario. Instead, the essential features of iDM are most directly probed by heavy target experiments, as discussed in section IV.

II. PARAMETER SPACE

Having explored the qualitative changes that arise from iDM, we can now proceed to a quantitative analysis of the allowed parameter space. It is difficult to perform a complete analysis as energy dependence is quite impor-

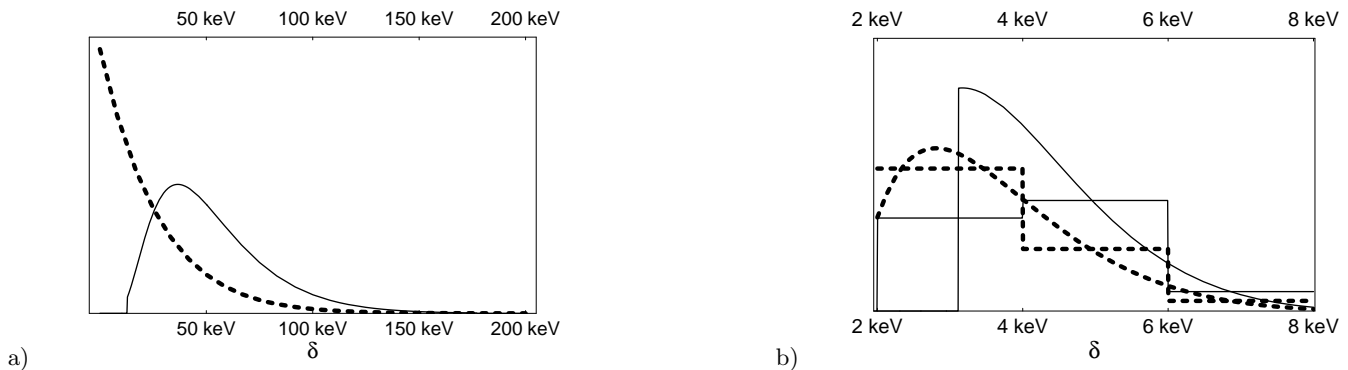


FIG. 3: a) The spectrum of signal at a germanium experiment as a function of energy, with area normalized to one. Shown are $m_\chi = 100\text{GeV}$ with $\delta = 80\text{keV}$ compared with the elastic scattering case. b) Spectrum of the modulated signal at DAMA for $m_\chi = 90\text{GeV}$ and $\delta = 140\text{keV}$ compared with the elastic case. In both cases, the thin, solid line is the inelastic case, and the dashed, thick line is the elastic case. The sharp cutoff in b) arises due to the finite galactic escape, and would be smoothed with a more realistic cutoff. The histogram shows the integrated signal in the corresponding bins, which is less sensitive to the details of the cutoff.

tant in the IDM scenario, and we lack the full details of the energy spectra obtained experimentally. As such, we will use the following limits for our analysis, which are consistent with published results from DAMA, Edelweiss and CDMS and CRESST, and with preliminary results presented from ZEPLIN-I.

In previous analyses we simply used the DAMA 3σ signal in the 2-6 keV region to set our parameters. Now, however, DAMA has given results for both the 2-4 keV region and the 4-6 keV region. We can extrapolate the 4-6 keV region by subtracting off the 2-4 keV signal, and assuming the 2-6 keV error comes from adding the two errors in quadrature. This approach assumes that the systematic effects from the two regions are the same, which is quite reasonable. Ultimately, we take 0.0466 ± 0.0094 cpd/kg integrated in the 2-4 keV bins, which is the value given in [2], and 0.0302 ± 0.0081 cpd/kg in the 4-6 keV bins, which is the extracted value. Using these values, we construct a χ^2 function that depends on the WIMP mass, δ , and σ_n . In figures 5 we indicate

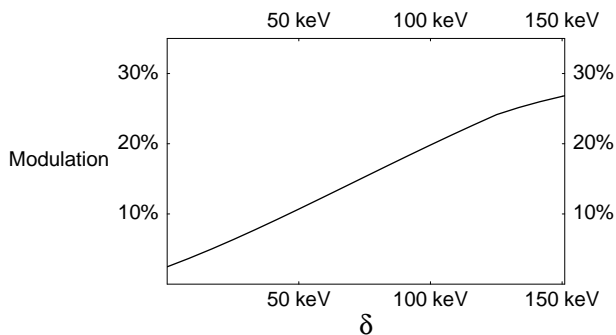


FIG. 4: Amplitude of modulation as a percentage of the unmodulated signal at DAMA as a function of δ , with $m_\chi = 90\text{GeV}$.

regions in δ - σ_n space with $\chi^2 < 4, 9$ for various WIMP masses.

The advantage of this technique is that we can begin to use the DAMA spectral information to see what regions of parameter space are preferred. DAMA also gives a limit on the maximum oscillation in the higher energy bins of -0.009 ± 0.0019 cpd/kg/keV. This places no constraint on the parameter space until very high cross sections ($\sigma_n > 10^{-36}$). We should note that the DAMA experiment has performed their own fit of the IDM scenario [2, 15], but in this analysis various nuclear and halo uncertainties are projected onto the parameter space. As we wish to compare experiments, we work in a single model, without varying the parameters. Earlier analyses had used previous limits from the DAMA pulse shape discrimination, NaI and Xe data. Here, we find this data is subsumed by the ZEPLIN-I limits and do not include it.

For CDMS we require an expectation of fewer than two events in 19.4 kg day of exposure in the energy interval above 10keV. We do not include Edelweiss at this time since CDMS is the most constraining Ge experiment. ZEPLIN-I has no published results, but has provided preliminary results both at idm 2002 [6] and TAUP in 2003 [5]. Although detailed limits on how many counts would be allowed do not exist, we can simply normalize our limits to those from ZEPLIN-I at $\delta = 0$. Their lowest excluded point lies at approximately $m_\chi \simeq 70\text{GeV}$ and $\sigma_n \simeq 10^{-42} \text{cm}^2$. Note that due to the enhanced modulation of this scenario, the sensitivity of the ZEPLIN experiment depends a great deal on the dates of their data taking. The impact can be a factor of two between summer data and winter data. Our limits assume the average, but have approximately 40% uncertainty for large δ . For CRESST, which is presently background-limited, we use the results presented in [7], and, as with ZEPLIN, normalize our results to the limit in the elastic case, which we take to be $\sigma_n < 1.6 \times 10^{-42} \text{cm}^2$ at $m_\chi = 70\text{GeV}$.

We combine these limits in figures 5 a-e for $m_\chi = 75, 100, 120, 250, 500$ GeV. These plots are affected somewhat by value used for v_0 , which is not a precisely measured quantity. In general, smaller values of v_0 tend to expand the allowed parameter space, and larger values tend to reduce it. These figures should certainly be viewed for their qualitative features primarily, as our use of constraints obtained in the elastic case to determine the constraints for the inelastic case is suspect. In particular, since traditional WIMP signals peak at low energies, an experiment may be able to place strong limits on a WIMP signal, even with higher background at intermediate energies. Since the expected signal for the iDM scenario is in the intermediate energy range, normalizing our limits to the elastic case would then *overstate* the limits for the inelastic case.

Note that the regions preferred by DAMA are disjoint. For example, for $m_\chi = 100$ GeV, there are points with $\chi^2 < 4$ for very small values of δ , and also for large values around $\delta = 120$ keV, but not for intermediate values around $\delta = 50$ keV. This is due to the effects of the annual modulation and the inelasticity of the scattering. For large values of δ , the signal is suppressed at low energies due to the inelasticity. For very small values of δ , the modulated signal (although not the rate itself), is also suppressed at low energies. However, at intermediate values of δ , the modulated signal is instead peaked at the minimum energy, 2 keV, so a cross section that leads to consistency with the data in the lower energy bin tends to give too large a modulated signal in the higher energy bin.

Under the assumption that this effect is at most order one, we see from figures 5 that ZEPLIN and especially CRESST have placed interesting constraints on the scenario. However, parameter space still exists which is consistent with all experiments simultaneously. Higher values of m_χ are somewhat less constrained than lower values. CDMS, with its new results, is competitive with the heavy target experiments at moderate values of δ , but will not be able to exclude the scenario, even with significantly more data, due to the effect of the finite galactic escape velocity. Later we shall see that CDMS still should see a sub-dominant elastic signal in the case that the iDM particle is a mixed sneutrino.

III. MODEL OF INELASTIC DARK MATTER

Models of iDM were discussed previously [11], but we review the basic approach to model building, and then discuss the “mixed sneutrino” case in order to focus our attention to regions of parameter space where one might expect a relic abundance consistent with observations.

Models of iDM are actually quite simple to construct. We begin by considering the case of a massive Majorana fermion. The simplest way to have a weakly interacting particle scatter off of a nucleus is to have it interact via exchange of a virtual Z-boson. However, massive Majorana

fermions do not carry conserved charges, and thus do not have vector couplings to gauge bosons. Yet we know that massive Dirac fermions, such as a fourth generation neutrino, can have such couplings, and a Dirac fermion is nothing more than two Majorana fermions. Hence we can deduce that a vector coupling must allow a transition of one Majorana fermion into another. If the gauge symmetry is broken, these states can be split from one another, and this splitting provides the small inelasticity needed for the framework.

Let us consider the case of fourth generation neutrino more carefully and see how this arises. Take $\psi = \begin{pmatrix} \eta \\ \bar{\xi} \end{pmatrix}$, with vector and axial-vector couplings to quarks:

$$\bar{\psi}\gamma_\mu(g'_V + g'_A\gamma_5)\psi\bar{q}\gamma^\mu(g_V + g_A\gamma_5)q. \quad (8)$$

This term would arise from integrating out massive gauge bosons. The dominant contribution to the scattering of ψ off of nuclei at a realistic dark matter experiment will come from the vector-vector piece, with an amplitude that scales approximately as the number of nucleons. The axial-axial piece couples to spin, and has no enhancement from the large number of nucleons.

Such a fourth-generation neutrino would require a Dirac mass ~ 100 GeV for ψ , but after electroweak symmetry breaking, we can also include a small Majorana mass term $\frac{\delta}{2}(\eta\eta + \bar{\eta}\bar{\eta})$, with $\delta \sim 100$ keV. The mass eigenstates are Majorana fermions given by

$$\chi_1 \simeq \frac{i}{\sqrt{2}}(\eta - \xi) \quad m_1 = m - \delta \quad (9)$$

$$\chi_2 \simeq \frac{1}{\sqrt{2}}(\eta + \xi) \quad m_2 = m + \delta. \quad (10)$$

The vector current, which will dominate if kinematically accessible, couples χ_1 to χ_2 , with the elastic scattering coupling suppressed by $\sim \delta/m$:

$$\bar{\psi}\gamma_\mu\psi \simeq i(\bar{\chi}_1\bar{\sigma}_\mu\chi_2 - \bar{\chi}_2\bar{\sigma}_\mu\chi_1) + \frac{\delta}{2m}(\bar{\chi}_2\bar{\sigma}_\mu\chi_2 - \bar{\chi}_1\bar{\sigma}_\mu\chi_1). \quad (11)$$

Choosing a Majorana mass splitting of order 100keV, we have arrived at precisely the inelastic scenario.

A. Mixed sneutrino iDM

Although the heavy neutrino provides a nice illustration of how the iDM scenario can be realized, in general its relic abundance is too small. However, in supersymmetric theories, a sneutrino can easily mix through A-terms with a singlet scalar to form “mixed” sneutrino dark matter [18]. Such scenarios can address the origin of neutrino mass [18, 19, 20], and have a significant impact on collider physics [21]. Since the lightest mass eigenstate is a linear combination of active and singlet particles, its couplings can be suppressed, and an acceptable relic abundance is easily achieved. We refer the reader to [18] for details.

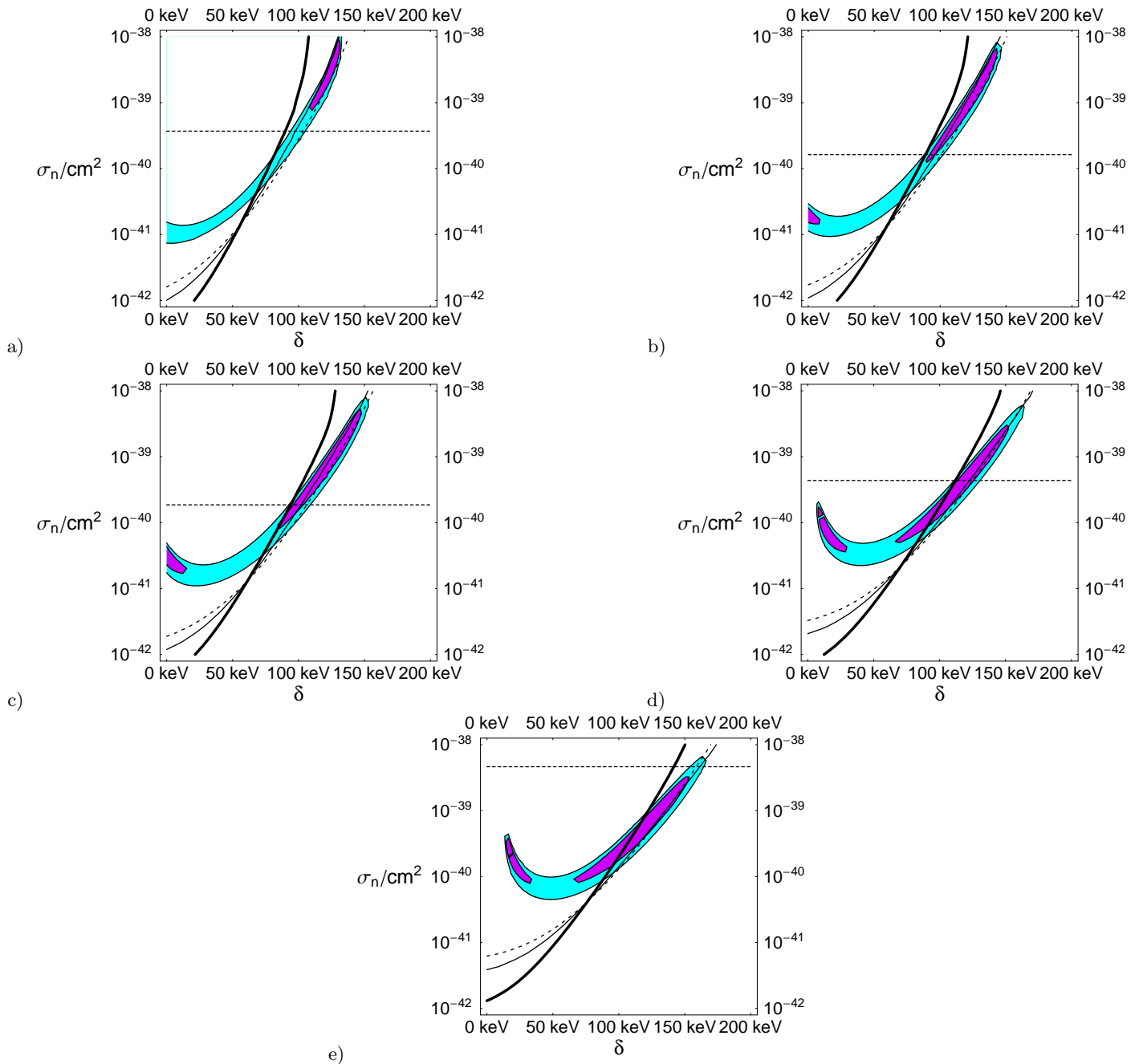


FIG. 5: Allowed regions in σ_n, δ parameter space for $m_\chi =$ a) 75 GeV b) 100 GeV c) 120 GeV, d) 250 GeV e) 500 GeV. The light and dark shaded regions have $\chi^2 < 9, 4$ as described in the text. The thick solid line is the CDMS limit. The dashed, curved line gives the CRESST results, and the thin solid line gives the preliminary ZEPLIN-I limit. The horizontal dashed line applies to the mixed sneutrino model, and is the upper bound on σ_n derived by considering the relic abundance, as described in the text.

Just as we can split a Dirac fermion into two inelastically scattering Majorana fermions, we can split a complex scalar (the lightest mass eigenstate) into two inelastically scattering real scalars. Both possibilities arise from an elastic scattering between degenerate states, which are then split by a small symmetry breaking parameter. This mechanism was first employed in the context of dark matter by [14], where the setup of [22] with

an unmixed sneutrino was considered as a possibility for dark matter. There, the splitting of scalar and pseudo-scalar states was used to suppress the annihilation rate of sneutrinos in the early universe, so that a cosmologically interesting relic abundance would result. The splitting required for this purpose was quite large, $\delta > 5$ GeV, making such a setup incompatible with the iDM scenario, leaving instead a traditional WIMP scattering via

Higgs exchange. However, in the mixed sneutrino setup, the relic abundance is controlled by a mixing angle $\sin\theta$, which specifies what fraction of the light state is active. Because of this mixing, a value of δ appropriate for the iDM scenario is viable, and can even arise quite naturally [18].

In calculating the relic abundance, contributions to the annihilation rate from Higgs and neutralino exchange depend significantly on details of the model. On the other hand, the interactions with gauge bosons relate directly to the cross section for scattering off of nuclei, and we can obtain upper bounds on the relic abundance by studying the corresponding contributions to the annihilation rate. That is, we obtain robust constraints by considering only annihilation through gauge interactions, while decoupling the other superpartners and the Higgs. Below m_W , one necessarily has annihilation via s-channel Z to fermions. This is a p-wave interaction, but still requires a $\sin^4\theta$ suppression to achieve a proper relic abundance. For larger masses, annihilation into W and Z pairs dominates. For sneutrinos near threshold, these channels can significantly suppress relic abundances, while for sneutrinos that are 500 GeV or heavier, even $\sin^4\theta = 1$ is allowed [23]. This is an interesting point: at about 500 GeV an ordinary (i.e., unmixed) sneutrino can have the proper relic abundance, and for $\delta \sim 150$ keV, such a WIMP is apparently still consistent with all data.

For a given sneutrino mass, the requirement that the sneutrino relic abundance be large enough leads to an upper bound on σ_n . To calculate this bound we take A-terms of 10 GeV and 40 GeV, respectively, for sneutrino masses of 120 GeV and 250 GeV (for lighter sneutrinos the abundance is independent of the A-term; for heavier ones $\sin^2\theta = 1$ is allowed). These upper bounds on σ_n appear as the horizontal lines in the figures. We have set the relic abundance to $\Omega h^2 = 0.1$ in accordance with various recent results. The overall normalization of the y-axis is uncertain at least to a factor of two, due to the overall uncertainty in the local dark matter density [24], which we incorporate by shifting the sneutrino abundance line up by a factor of two in the cross section space. Note that for smaller values of m_χ , the relic abundance calculation suggests that there is very little room for mixed-sneutrino iDM, but that the situation improves for larger values of the mass.

IV. FUTURE EXPERIMENTS AND ELASTIC SCATTERING SIGNATURES

In the short term, we expect additional results from xenon, germanium and tungsten experiments. A significant improvement of the sensitivity of the heavy target experiments should certainly confirm or exclude this scenario. The new CDMS results have once again made it competitive with the heavy targets in the moderate δ range, and continued improvement could exclude this

region. However, this depends sensitively on the escape velocity of the galaxy. If it is too low, and δ is too large there may be no signature at all from inelastic scattering at germanium experiments.

Nonetheless, at least for the sneutrino model we have focused on, Ge experiments may still detect the WIMP through its *elastic* scattering. Although elastic scattering via Z exchange is suppressed, there is still the possibility of scattering via Higgs exchange, with cross section [18]

$$\sigma_n = \left(\frac{(m_{heavy}^2 - m_{\tilde{\nu}}^2) \sin^2(2\theta) - 2\sqrt{2}m_Z^2 \cos(2\beta) \sin^2(\theta)}{200\text{GeV} \times v} \right)^2 \times \left(\frac{100\text{GeV}}{m_{\tilde{\nu}}} \right)^2 \left(\frac{115\text{GeV}}{m_h} \right)^4 (3 \times 10^{-43} \text{cm}^2). \quad (12)$$

here, m_{heavy}^2 is the mass squared of the heavy linear combination of active and singlet sneutrinos. There is great uncertainty in the strange quark content of the nucleon [25], which makes the precise value of the cross section uncertain. Still, upcoming results from CDMS Soudan should be able to test this model, even in the event that δ is so large that no inelastic scatterings occur.

V. CONCLUSIONS

We have reexamined the framework of inelastic dark matter in light of recent data from Edelweiss, DAMA, CDMS Soudan, ZEPLIN-I and CRESST. We find that these experiments have placed interesting constraints on the parameter space of the framework, but that there are still regions which accommodate all experimental results. If δ is very large, a significant spectrum deformation should be seen in the present DAMA data and in future LIBRA data, but CDMS may see nothing. If δ is small, CDMS should see spectral distortion, with low energy events suppressed. In all cases, upcoming experiments with heavy targets such as ZEPLIN and CRESST should unambiguously test this scenario.

Building models of iDM is quite simple, with fourth generation neutrinos and mixed sneutrinos interesting possibilities. In the sneutrino model, the parameter space is restricted, but still viable. CDMS Soudan should be capable of testing this model through its elastic scattering via Higgs exchange, even in the event that δ is too large to allow inelastic scattering off of Ge.

Acknowledgments The work of NW was partially supported by the DOE under contracts DOE/ER/40762-213 and DE-FGO3-96-ER40956, and the work of DT-S was supported by a Research Corporation Cottrell College Science Award.

-
- [1] D. N. Spergel et al., *Astrophys. J. Suppl.* **148**, 175 (2003), astro-ph/0302209.
- [2] R. Bernabei et al. (2003), astro-ph/0311046.
- [3] D. S. Akerib et al. (CDMS) (2004), astro-ph/0405033.
- [4] G. Gerbier (2003), talk at TAUP 2003, Seattle, WA, USA.
- [5] N. Smith (2003), talk at TAUP 2003, Seattle, WA, USA.
- [6] N. Smith (2002), talk at idm 2002, York, UK.
- [7] G. Angloher et al. (2004), astro-ph/04080006.
- [8] C. J. Copi and L. M. Krauss, *Phys. Rev.* **D67**, 103507 (2003), astro-ph/0208010.
- [9] P. Ullio, M. Kamionkowski, and P. Vogel, *JHEP* **07**, 044 (2001), hep-ph/0010036.
- [10] A. Kurylov and M. Kamionkowski, *Phys. Rev.* **D69**, 063503 (2004), hep-ph/0307185.
- [11] D. R. Smith and N. Weiner, *Phys. Rev.* **D64**, 043502 (2001), hep-ph/0101138.
- [12] R. Bernabei et al. (DAMA), *Phys. Lett.* **B480**, 23 (2000).
- [13] D. R. Smith and N. Weiner, *Nucl. Phys. Proc. Suppl.* **124**, 197 (2003), astro-ph/0208403.
- [14] L. J. Hall, T. Moroi, and H. Murayama, *Phys. Lett.* **B424**, 305 (1998), hep-ph/9712515.
- [15] R. Bernabei et al., *Eur. Phys. J.* **C23**, 61 (2002).
- [16] J. Engel, *Phys. Lett.* **B264**, 114 (1991).
- [17] C. S. Kochanek, *Astrophys. J.* **457**, 228 (1996), astro-ph/9505068.
- [18] N. Arkani-Hamed, L. J. Hall, H. Murayama, D. R. Smith, and N. Weiner, *Phys. Rev.* **D64**, 115011 (2001), hep-ph/0006312.
- [19] F. Borzumati and Y. Nomura, *Phys. Rev.* **D64**, 053005 (2001), hep-ph/0007018.
- [20] N. Arkani-Hamed, L. J. Hall, H. Murayama, D. R. Smith, and N. Weiner (2000), hep-ph/0007001.
- [21] C. L. Chou, H. L. Lai, and C. P. Yuan, *Phys. Lett.* **B489**, 163 (2000), hep-ph/0006313.
- [22] Y. Grossman and H. E. Haber, *Phys. Rev. Lett.* **78**, 3438 (1997), hep-ph/9702421.
- [23] T. Falk, K. A. Olive, and M. Srednicki, *Phys. Lett.* **B339**, 248 (1994), hep-ph/9409270.
- [24] M. Kamionkowski and A. Kinkhabwala, *Phys. Rev.* **D57**, 3256 (1998), hep-ph/9710337.
- [25] A. Kryjevski (2003), hep-ph/0312196.